Evaluating Size-Specific Dose Estimate (SSDE) as an Estimate of Organ Doses from Routine CT Exams Derived from Monte Carlo Simulations

Anthony J. Hardy, PhD[1*]; Maryam Bostani, PhD[2,3]; Hyun J. Kim, PhD[2]; Chris Cagnon, PhD[2,3]; Maria Zankl, MSc[4]; Michael McNitt-Gray, PhD[2,3]

Running title: SSDE as estimates of Organ Doses

[1]Livermore National Laboratory, Materials Engineering Division/Non-destructive Evaluation Group, Livermore, CA, 94550

[2]Department of Radiological Sciences, David Geffen School of Medicine, University of California, Los Angeles, Los Angeles, Livermore, 90024

[3]Physics and Biology in Medicine Graduate Program, David Geffen School of Medicine, University of California, Los Angeles, Los Angeles, California, 90024

[4]Helmholtz Zentrum München, German Research Center for Environmental Health (GmbH), Institute of Radiation Medicine, Ingolstaedter Landstrasse 1, Neuherberg 85764, Germany

***Corresponding Author**
ajhardy06@gmail.com

ABSTRACT

Purpose

The size specific dose estimate (SSDE) is a metric that adjusts $CTDI_{vol}$ to account for patient size. While not intended to be an estimate of organ dose, AAPM Report 204 notes the difference between the patient organ dose and SSDE is expected to be 10-20%. The purpose of this work was therefore to evaluate SSDE against estimates of organ dose obtained using Monte Carlo (MC) simulation techniques applied to routine exams across a wide range of patient sizes.

Materials and Methods

SSDE was evaluated with respect to organ dose based on representative organs for each of three routine protocols: (1) brain parenchyma dose in routine head exams; (2) lung and breast dose in routine chest exams; and (3) liver, kidney, and spleen dose in routine abdomen/pelvis exams. For each exam, voxelized phantom models were created from existing models or derived from clinical patient scans. For routine head exams, 15 patient models were used which consisted of 10 GSF/ICRP voxelized phantom models and 5 pediatric voxelized patient models created from CT image data. For the routine chest exams, data from 161 patients were collected with a D_w range of ~16 to 44 cm. For the routine abdomen/pelvis exams, data from 107 patients were collected with a range of D_w from ~16 to 44 cm. Image data from these patients were segmented to generate voxelized patient models. For routine head exams, fixed tube current (FTC) was used while tube current modulation (TCM) data for body exams were extracted from raw projection data. The voxelized patient models and tube current information were used in detailed MC simulations for organ dose estimation. For all exams, the size metric used was water equivalent diameter (D_w). Organ doses from MC simulation were normalized by $CTDI_{vol}$ and parameterized as a function of D_w. For each patient scan, the SSDE was obtained using D_w and $CTDI_{vol}$ values of each scan, according to AAPM Report 204 for body scans and Report 293 for head scans. For each protocol and each patient, normalized organ doses were compared to SSDE. A one-sided tolerance limit covering 95% (p = 0.95) of

the population with 95% confidence (α = 0.05) was used to assess the upper tolerance limit (T_U) between SSDE and normalized organ dose.

Results

For head exams, the T_U between SSDE and brain parenchyma dose was observed to be 12.5%. For routine chest exams, the T_U between SSDE and lung and breast dose was observed to be 35.6% and 68.3%, respectively. For routine abdomen/pelvis exams, the T_U between SSDE and liver, spleen, and kidney dose was observed to be 30.7%, 33.2%, and 33.0%, respectively.

Conclusions

The T_U of 20% between SSDE and organ dose was found to be insufficient to cover 95% of the sampled population with 95% confidence for all of the organs and protocols investigated, except for brain parenchyma dose. For the routine body exams, excluding the breasts, a wider threshold difference of ~30-36% would be needed for the coverage and confidence investigated in this study.

Keywords: Size-specific dose estimate, Monte Carlo dose simulations, TCM, routine CT exams

1. INTRODUCTION

CT is widely used as a diagnostic tool due to its ability to acquire cross-sectional images of patient anatomy in a relatively short amount of time. In 2006, abdominal/pelvic, head, and chest CT scans conducted within the United States accounted for 32%, 28%, and 16%, respectively, of all CT procedures [1]. Additionally, the 2015 UC DOSE study found that, across twelve University of California medical centers, abdominal/pelvic, chest, and head scans accounted for 32%, 16%, and 13% of all adult CT procedures [2]. Routine examinations may be reasonably assumed to comprise the large majority of these CT procedures. Thus, patient organ dose assessments from routine procedures are of substantial interest.

The volumetric Computed Tomography Dose Index ($CTDI_{vol}$) and dose-length product (DLP), two commonly-reported CT dose metrics, are understood to not necessarily be indicative of patient dosimetry [3]. This is primarily due to the differences in composition and geometry of the CTDI phantom relative to a human patient. There are at present two ways of estimating patient organ dose from CT: (1) in vitro empirical dose measurements using dosimeters such TLDs or MOSFETs within anthropomorphic phantoms or cadavers and (2) dose calculations from MC software packages.

Both of these approaches have inherent advantages and disadvantages in the current context of modern CT dosimetry. In brief, in vitro empirical measurements are advantageous in that dose estimates come directly from the CT source, meaning that specific automatic exposure control (AEC) strategies of manufacturers are captured in these dose readings, provided that the dosimeters are properly calibrated. In addition, this method does allow for repeated exposures. A drawback to physical measurements, however, is that oftentimes even the most sophisticated anthropomorphic phantoms models, such as the CIRS phantoms [4] and even cadavers [5], may not have the breadth to be reflective of the range of actual patient anatomy experienced clinically. In vivo measurements can be done, such as in the study where TLDs were placed in the colon and used for CT colonography dosimetry [6]. However, in vivo measurements are often invasive. Moreover, the dose distribution within the patient is not necessarily uniform, particularly near the surface of a patient [7]. Therefore, adequate spatial sampling of the non-uniform distribution to obtain an estimate of organ dose may require a large number of dosimeters.

MC approaches address some of the shortcomings of the in vitro, empirical methods. MC methods obviate the need for dosimeters entirely due to the mathematical transportation of particles through a particular medium. Moreover, the availability of highly-sophisticated, deformable, mathematical phantoms models, such the XCAT family models [8], allows for permutations of human anatomy. Commercially-available dose management software packages, used widely in hospitals and medical centers, often employ MC simulations based on these sophisticated, mathematical models of human anatomy. However, this approach comes with its own set of challenges. As with any MC simulation, the accuracy of the MC approach is highly dependent upon the accuracy of the simulation set up [9], [10]. For CT dosimetry, this accuracy requires both sufficient scanner x-ray source descriptions and accurate representations of both vendor-specific AEC algorithms and patient anatomic representations. Furthermore, MC methods require extensive validation, usually with equivalent empirical measurements, and can be time prohibitive and computationally expensive.

While not originally intended to be a measure of organ dose, SSDE does have the potential to provide an accessible and quick estimate of organ dose in lieu of empirical measurement and MC approaches. Per Report 204, SSDE was based on fixed tube current (FTC) [11], [12]. A study conducted by Moore et al. investigated the correlation between absolute organ dose from TCM scans with SSDE in pediatric and adult patients using in vitro organ dose measurements from four CIRS anthropomorphic phantoms [13]. This study used effective diameter (*ED*) as the metric of patient and phantom size and compared patient organ dose derived from SSDE-to-organ dose conversion coefficients to published MC results of computational phantoms. The Moore et al. study found that the average correlation of SSDE and absolute organ dose was found to be within ± 10% of unity [13]. Another study conducted by Sinclair et al. compared correlations of $CTDI_{vol}$-normalized organ dose versus *ED* against SSDE for chest/abdomen/pelvis exams [14]. In this study, the organ dose values were from in vitro measurements of 8 cadavers representing a range of sizes from the University of Florida. In this study, the difference between the average overall organ dose measurements from the cadavers and SSDE ranged from -23% to 4% [14]. In both these studies, *ED* was used as the metric of patient size, whereas the attenuation-based

size metric water equivalent diameter (D_w) is now more commonly used [15]. Moreover, the Moore et al. study indirectly compared SSDE to empirical measurements and MC simulations of hybrid computational phantom models from Lee et al. and Li et al. [16], [17]. As mentioned above, the use of in vitro measurements from detailed physical phantoms and MC simulations of the highly-sophisticated computational phantom may not be representative of variation of patient habitus.

Therefore, the purpose of this study was to evaluate SSDE as an estimate of organ doses derived from the MC simulation of routine exams. In contrast to the previous studies, this evaluation of SSDE was performed on a direct, per-organ basis across a wide range of patient habitus for routine head, chest, and abdomen/pelvis exams. Specifically, this study evaluated the SSDE in relation to brain parenchyma dose from routine head exams; lung and breast dose from routine chest exams; and liver, spleen, and kidney dose from routine abdomen/pelvis exams.

2. MATERIALS AND METHODS

2.A Voxelized patient cohorts

2.A.1 Routine Head Exams

The patient data for the routine head exams was from Hardy et al [18]. This data consists of a total of 15 voxelized patient models. Ten voxelized phantom models from the GSF (Helmholtz Zentrum München, German Research Center for Environment Health, Institute of Radiation Protection, Neuherberg, Germany) family [19] and the ICRP (International Commission Radiological Protection) voxelized reference male and female [20], [21] were used. These models had all radiosensitive organs identified. The eight GSF voxel-based models were generated from CT images with up to 131 organs and anatomic structures segmented. Two of the voxelized models were the ICRP reference male and female models. They were each based on modifications of two corresponding male and female GSF models of similar external dimensions. The GSF/ICRP voxelized models used in this study had the in-plane resolution subsampled from the original by approximately a factor of four or eight to decrease computation time [19]–[21]. The remaining five patient models were derived from pediatric patient data

in order to extend the pediatric size range. These data sets were collected from clinically-indicated scans under IRB approval.

The routine head protocols were performed with FTC. The details of the protocol are listed in **Table 1**. Because the analyses will be performed on a per mAs basis, the $CTDI_{vol,16}$/mAs value is reported.

Table 1: Routine helical head scanning protocol and associated $CTDI_{vol,16}$ per mAs for the scan from Hardy et al [18]

Parameter	Setting
kV	120
Rotation time (s)	0.5
Helical pitch	0.55
Nominal collimation (mm)	28.8
Bowtie filter	Standard
$CTDI_{vol,16}$/mAs (mGy/mAs)	0.24

2.A.2 Routine Chest Exams Patient Cohort

To estimate lung and glandular breast tissue dose from routine chest exams, data were collected under IRB approval from 161 patients undergoing clinically indicated CT exams (19 pediatric females, 23 pediatric males, 53 adult females, 65 adult males) with a range of D_w values from 16 to 44 cm. The routine chest examinations were performed using tube current modulation (TCM). Data were collected from four different scanners: Sensation 16 (S16), Sensation 64 (S64), Definition AS64, and SOMATOM Force (all from Siemens Healthineers, Forchheim, Germany). **Table 2** summarizes the scanning protocols for the routine chest protocols used for the four scanners. Because of the presence of pediatric and bariatric patients, some alterations of the routine chest protocol—such as reduced tube voltage for pediatric patients, reduced pitch for bariatric patients ($D_w \approx 40$ or greater), and different bowtie filters for pediatric patients—were present in this cohort. All scans were performed with TCM (CAREDose4D, Siemens Healthineers, Germany) with the CAREDose4D Quality Reference mAs (QRM) value as described in **Table 2** and strength set to "Average." For all cases, the TCM data was extracted from the

raw projection data that was collected at the time of the scan. The chest scans were all performed in the supine position. Image data were reconstructed at 500 mm field-of-view (FOV) in order to ensure patient anatomy is contained within the FOV. For bariatric patients, portions of peripheral anatomy were often still outside of the 500 mm FOV. In these cases, an extended FOV (eFOV) of 650 mm was employed to encompass the anatomy for larger patients. **Table 3** summarizes the quantity of patient data from each scanner.

Table 2: Routine chest scanning parameters for the four scanners used in this investigation

Parameter	S16	S64	AS64	Force
kV*	100	120	120	120
Quality reference mAs (QRM)	140	140	140	140
Rotation time (s)	0.5	0.5	0.5	0.5
Pitch†	1.0	1.0	1.0	1.0
Nominal collimation (mm)	24.0	19.2	19.2	57.6
Bowtie filter‡	Body	Body	Body/W1	Body/W1

* Most of the pediatric patients were scanned with 100 kV.
†Bariatric patients were scanned with pitches lower than 1.0
‡For the AS64 and Force scanners, the pediatric patients were scanned with Head/W2 bowtie filter

Table3: Overview of chest scans collected from the different scanners used in this study

Patient cohort	S16	S64	AS64	Force	Total
Adult males	-	42	12	11	65
Adult females	-	29	12	12	53
Pediatric males	6	12	5	1	24
Pediatric females	7	5	7	0	19
Total	13	88	36	24	161

To use the patient image data for MC simulations, patient anatomy contained within the image data were voxelized. Voxels within the image data were modeled as either lung, fat, water, muscle, bone or air then subdivided into one of seventeen density levels in relation to their CT number [22], [23]. The lung tissue was semi-automatically contoured in both female and male patients; glandular breast tissue, however, was only segmented for female patients [24]. **Figure 1** contains examples of segmented male and female patient image data and resulting voxelized models.

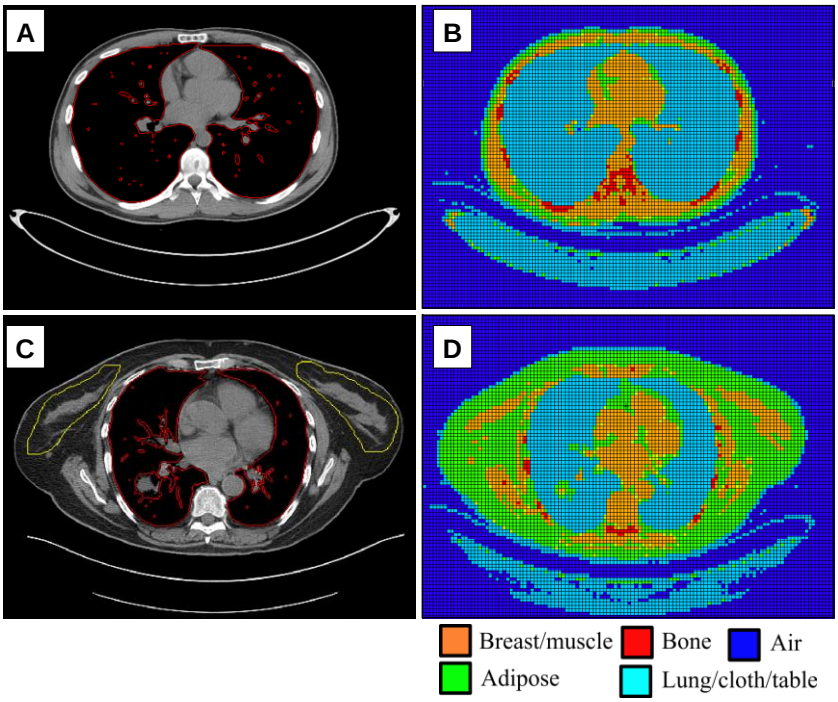

Figure 1: A) Segmented images of a male patient who underwent clinically-indicated chest CT exam with **B)** the voxelization of the segmented image data for use in MC simulations. In **A)**, only the lung tissue (red outline) is segmented. **C)** Segmented images of a female patient who underwent clinically-indicated chest CT exam with **D)** the voxelization of the segmented image data for use in MC simulations. In **C)**, both lung (red outline) and glandular breast tissue (yellow outline) are segmented.

2.A.3 Routine Abdominal/Pelvic Exams

To estimate liver, spleen, and kidney dose from routine abdomen/pelvis exams, data were collected under IRB approval from 107 patients undergoing clinically indicated CT exams (9 pediatric females, 12 pediatric males, 44 adult females, 42 adult males) with a range of D_w values from 16 to 44 cm. The routine abdomen/pelvis examinations were performed using TCM. Data were collected from three different scanners: Sensation 64 (S64), Definition AS64, and SOMATOM Force (all from Siemens Healthineers, Forchheim, Germany). As with the routine chest protocol in Sec. 2.A.2, some alterations of the routine abdomen/pelvis protocol were present in this cohort because of the presence of pediatric and bariatric patients (again, defined as $D_w \approx 40$ or greater). All scans were performed with TCM (CAREDose4D, Siemens Healthineers, Germany) with the QRM value as described in **Table 4** and

strength set to "Average." For call cases, the TCM data was extracted from the raw projection data that was collected at the time of the scan. **Table 4** contains the remaining scanning parameter for the abdomen/pelvis protocols for the three scanners of this investigation. All of the abdomen/pelvis scans were performed in the supine position, and the image data were reconstructed at 500 mm field-of-view (FOV) in order to ensure patient anatomy is contained within the FOV. An extended FOV (eFOV) of 650 mm was utilized to encompass the anatomy for bariatric patients. **Table 5** summarizes the quantity of patient data from each scanner. The abdominal/pelvic image data were voxelized for utilization in MC simulations in the same manner as Sec 2.A.2 above. **Figure 2** contains examples of segmented female patient image data and resulting voxelized models.

Table 4: Routine abdominal/pelvis scanning parameters for the three scanners used in this investigation

Parameter	S64	AS64	Force
kV*	120	120	120
Quality reference mAs (QRM)	180	180	180
Rotation time (s)	0.5	0.5	0.5
Pitch†	1.0	1.0	1.0
Nominal collimation (mm)	19.2	19.2	57.6
Bowtie filter‡	Body	Body/W1	Body/W1

* Most of the pediatric patients were scanned with 100 kVp.
†Bariatric patients were scanned with pitches lower than 1.0
‡For the AS64 and Force scanners, the pediatric patients were scanned with Head/W2 bowtie filter

Table 5: An overview of abdomen/pelvis scans collected from the different scanners used in this study

Patient cohort	S64	AS64	Force	Total
Adult males	30	8	4	42
Adult females	32	7	5	44
Pediatric males	11	-	1	12
Pediatric females	9	-	0	9
Total	82	15	10	107

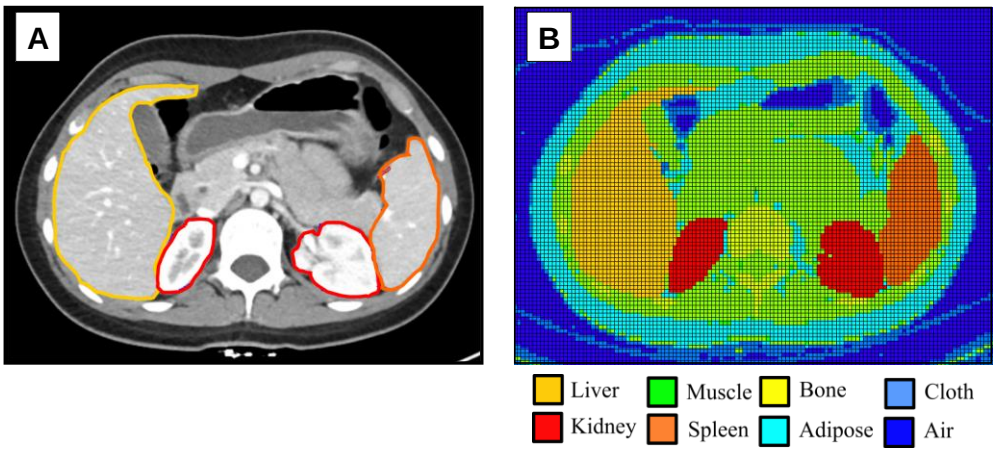

Figure 2: A) Segmented images of a female patient who underwent clinically-indicated abdomen/pelvis CT exam with **B)** the voxelization of the segmented image data for use in MC simulations.

2.B. Patient size metrics

Water equivalent diameter (D_w) was chosen as the metric of patient for this investigation. AAPM Report 220 describes two methods of estimating D_w: one based on values extracted from the topogram and one based on CT image data [15]. For this study, both approaches were used, depending on the data available. For those patients whose data was collected on either the Sensation 16 or the Sensation 64 scanners, estimates of D_w were based on the CT numbers in the image data. This was done because the CT scan radiographs (i.e. topograms) for these patients were not available. Specifically, D_w was estimated at the center of the image series using the methods outlined in AAPM Report 220 for assessing D_w from CT numbers in image data [25]. For the patients whose data was gathered from the Definition AS64 or the Force scanners, estimates of D_w were extracted from the topogram. For each patient model, D_w was assessed at the longitudinal center of the image series while the estimates of D_w were obtained from the topogram at that center location. This method of acquiring D_w from the topogram is also based on the methodology outline in AAPM Report 220 wherein D_w is calculated using the lateral (LAT) and anterior-posterior (AP) measurements also found within the topogram [25].

2.C. MC simulations

The MC simulation package used for this study was MCNPX. Modifications to MCNPX allowed for the implementation of "equivalent source" and "equivalent bowtie" of the four MDCT scanners used in this investigation [26]. All simulations were performed in photon transport mode with a 1 keV low-energy cut-off. All simulations were performed with 10^7 particle histories to ensure a statistical uncertainty of less than 1%. In order to incorporate the TCM data into the MC simulation, the methods described by Angel et al. were used in that an additional text file containing the TCM information was generated by extracting the tube current information from the raw projection data [24]. In the text file, the tube current $I(z,\Theta)$ was expressed as a function of table position (z) and tube angle (Θ). MCNPX simulations were performed using the computational and storage services associated with the Hoffman2 Shared Cluster provided by UCLA Institute for Digital Research and Education's Research Technology Group.

2.D Dose Analysis

Absolute organ dose values were estimated from MC simulations by applying scanner-, tube voltage-, collimation-specific normalization factors [27]. $CTDI_{vol}$-normalized organ dose values (nD_{organ}) from the routine exams investigated were calculated by normalizing the absolute organ doses by $CTDI_{vol}$ values. $CTDI_{vol}$-normalized brain parenchyma dose values (nD_{brain}) from routine head exams were calculated using $CTDI_{vol,16}$. $CTDI_{vol}$-normalized lung and breast dose values (nD_{lung} and nD_{breast}) were calculated using $CTDI_{vol,32}$ for normalization. Similarly, $CTDI_{vol,32}$ was used to normalize liver, kidney, and spleen dose values (nD_{liver}, nD_{kidney}, and nD_{spleen}, respectively). All $CTDI_{vol}$ values were taken from the patient protocol page produced by the scanners utilized in this investigation. Lastly, each nD_{organ} was parameterized as an exponential function with respect to D_w using the same form as AAPM Report 204. Regression analyses were used to determine the coefficients of the exponential function for each scan protocol and organ.

2.E Statistical Analysis

nD_{organ} values from the routine exams were compared to SSDE *f*-factors (henceforth referred to as SSDE). This study used the SSDE from AAPM Report 293 for head exams and AAPM 204 for body exams as the basis of comparison [11], [12]. For an individual patient, $\Delta D_{SSDE,organ}$ is the nD_{organ} value relative to the SSDE value based on the patient's D_w estimate. This was calculated for each patient, for each protocol, and for each organ. The definition of $\Delta D_{SSDE,organ}$ for a given patient *i* is given by **Eq. 1**:

$$(\Delta D_{SSDE,organ})_i\ (\%) = \frac{(nD_{organ})_i - SSDE(D_w)_i}{SSDE(D_w)_i} \times 100\% \qquad \textbf{Eq. 1}$$

For each organ dose from each protocol, the average difference relative to SSDE ($\overline{\Delta D_{SSDE,organ}}$), and the standard deviation of the difference relative to SSDE ($\Delta S_{SSDE,organ}$) were calculated using **Eq. 2** and **Eq. 3**, respectively.

$$\overline{\Delta D_{SSDE,organ}}\ (\%) = \frac{1}{N}\sum_{i=1}^{N} |(\Delta D_{SSDE,organ})_i| \qquad \textbf{Eq. 2}$$

$$\Delta S_{SSDE,organ}\ (\%) = \sqrt{\frac{1}{N-1}\sum_{i=1}^{N}\left(|(\Delta D_{SSDE,organ})_i| - \overline{\Delta D_{SSDE,organ}}\right)^2} \qquad \textbf{Eq. 3}$$

Where *N* is the total number of patients.

A second analysis was performed to assess the number of cases where the estimated organ doses agreed with SSDE values to within a certain tolerance (either ± 20% and ± 30% of the SSDE). In the plots found in Sec. 3 below, this is graphically illustrated by using shaded regions that correspond to ± 20% and ± 30% of the SSDE. The proportion of the data points within these regions (C_p) were given for each organ and was calculated using **Eq. 4**.

$$C_p = \frac{\#\text{ of points within the regions relative to SSDE}}{N} \qquad \textbf{Eq.4}$$

Lastly, in order to determine the coverage of SSDE as an estimate of organ dose over a fixed proportion of the population, a one-sided, upper tolerance limit was calculated. The one-sided tolerance limit was

utilized because this study is concerned with assessing the upper tolerance limit (T_U) of the difference between normalized organ dose and the SSDE values. The coverage factor (proportion of the population of nD_{organ} values, p) used to construct the tolerance limit was 95% (p = 0.95) with a confidence level of 95% (α = 0.05). Using the upper bound of 20% difference between SSDE and patient dose mentioned in AAPM Report 204 as a point of comparison, the hypotheses for this study were as follows:

1) Null hypothesis (H_0): $T_U \leq 20\%$ with a confidence of 95% (α = 0.05) covering 95% of the population (p = 0.95).
2) Alternative hypothesis (H_1): $T_U > 20\%$ with a confidence of 95% (α = 0.05) covering 95% of the population (p = 0.95).

Where T_U is calculated as

$$T_U = \overline{\Delta D_{SSDE,organ}} + k_1(\alpha, p, N)\Delta S_{SSDE,organ} \qquad \textbf{Eq. 5}$$

Where is k_1 is the factor that determines the upper limit to cover proportion p with confidence (1-α)% using sample size N [28]. The upper tolerance limit of 30% difference between SSDE and patient dose can be derived analogously. **Figure 3** is the process workflow for evaluating SSDE against organ dose.

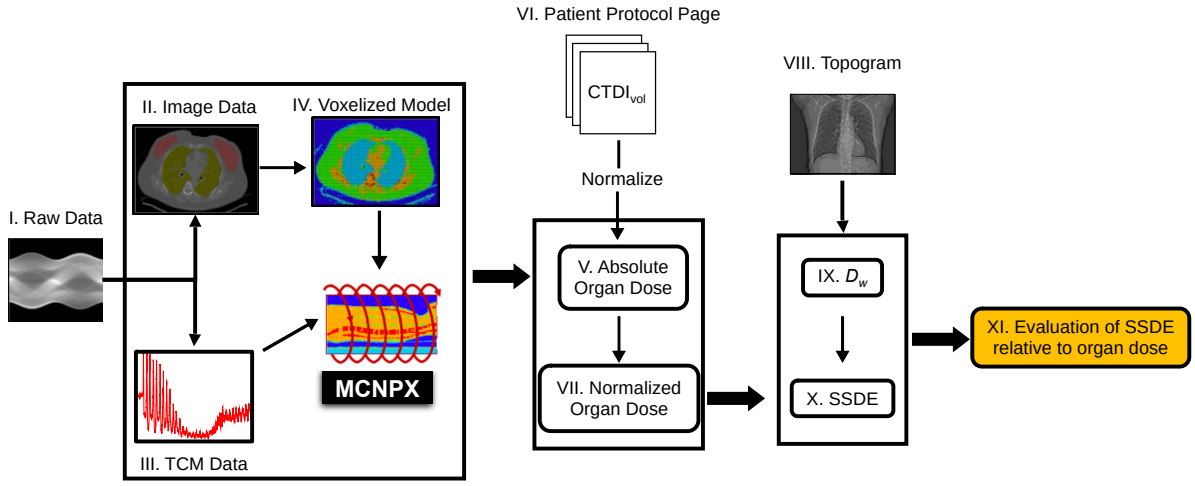

Figure 3: The workflow process for this study in the instances where raw projection data was needed. Starting with (I) raw projection data as input, (II) image data were reconstructed and segmented. (III) Tube current profiles was extracted from the raw data. (IV) The segmented image data was voxelized by mapping CT number to a material designation using a look-up table. The TCM data (III) and the voxelized patient model (IV) were incorporated into MCNPX to get (V) absolute organ doses. Absolute organ doses (V) were normalized by (VI) CTDI$_{vol}$ from the patient protocol page to yield (VII) CTDI$_{vol}$-normalized organ doses. (VIII) From the topogram, estimates of D_w (IX) were then extracted. In this workflow, D_w estimates can also be taken from the image data. The D_w estimates were used to calculate the SSDE (X) from AAPM Reports 204 and 220. Lastly SSDE was then evaluated (XI) relative to MC-derived CTDI$_{vol}$-normalized organ doses. Where raw projection data was not needed, such as for the routine head scans, I and III were skipped and CTDI$_{vol,16}$/mAs measurement was used in lieu of VI.

3. RESULTS

3.A SSDE relative to brain parenchyma dose from routine head exams

Table 6 below contains the D_w estimates, SSDE from AAPM Report 293, nD_{brain} values, and difference (%) of nD_{brain} values relative to the SSDE ($\Delta D_{SSDE,brain}$). In addition, the mean ($\overline{\Delta D_{SSDE,brain}}$) and standard deviation of brain dose relative to SSDE($\Delta S_{SSDE,brain}$) are also included in **Table 6**. The patient population did include both pediatric and adult patients with a range of D_w from ~11 to 20 cm. $\Delta D_{SSDE,brain}$ values ranged from -5.9% to 13.8%. $\overline{\Delta D_{SSDE,brain}}$ was observed to be 4.4% and $\Delta S_{SSDE,brain}$ was observed to be 3.2%. All 15 nD_{brain} values were within 20% of SSDE (C_p = 100.0%). Using N = 15, T_U for SSDE covering 95% of the population for nD_{brain} with 95% confidence was observed to be 12.5%.

Figure 4 shows below nD_{brain} parameterized as an exponential function with D_w in relation to SSDE values from AAPM Report 293.

Table 6: D_w estimates, SSDE, nD_{brain} values, and difference of nD_{brain} values relative to the SSDE ($\Delta D_{SSDE,brain}$) for the patients investigated

Name	D_w (cm)	SSDE	nD_{brain}	$\Delta D_{SSDE,brain}$ (%)
Peds2	12.6	1.07	1.12	-4.8
Peds1	10.6	1.19	1.17	1.4
Baby	11.1	1.16	1.16	-0.7
Peds3	15.6	0.93	0.98	-5.3
Peds5	17.1	0.86	0.81	5.5
Peds4	15.7	0.92	0.89	3.5
Child	17.2	0.86	0.91	-6.2
Helga	18.2	0.82	0.81	0.4
Irene	17.1	0.86	0.84	2.4
Golem	18.3	0.81	0.86	5.5
Visible Human	19.6	0.76	0.74	2.3
Regina	19.9	0.75	0.85	-13.8
Donna	18.7	0.79	0.83	5.0
Rex	20.2	0.74	0.78	5.4
Frank	19.2	0.78	0.73	5.9
			$\overline{\Delta D_{SSDE,brain}}$	4.4
			$\Delta S_{SSDE,brain}$	3.2
			T_U	12.5

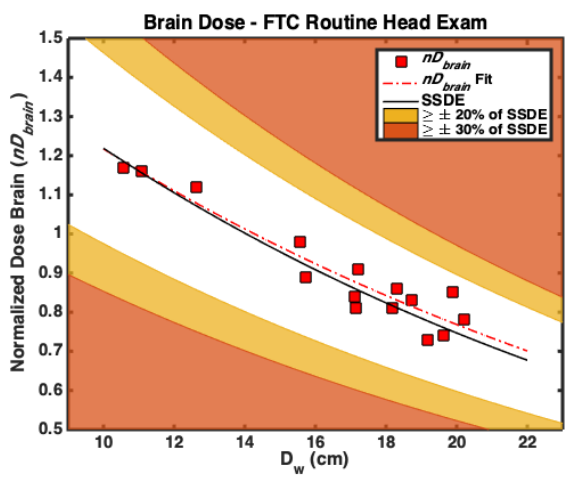

Figure 4: nD_{brain} values in relation to SSDE from AAPM Report 293 with shaded areas corresponding to ± 20% and ± 30% of the SSDE

3.B SSDE relative to lung and breast dose from routine chest exams

Figure 5A contains nD_{lung} parameterized as an exponential function with D_w in relation to SSDE from AAPM Report 204. For nD_{lung}, $\Delta D_{SSDE,lung}$ values ranged from -60.4% to 20.1%. $\overline{\Delta D_{SSDE,lung}}$ was observed to be 15.3% and $\Delta S_{SSDE,lung}$ was observed to be 10.9%. Of the 160 cases, 119 of the nD_{lung} values were within 20% of SSDE (C_p = 74.4%) while 148 of the nD_{lung} values were within 30% of SSDE (C_p = 92.5%). Only 12 of the nD_{lung} cases were beyond 30% of SSDE (C_p = 7.5%). Using N = 160, T_U for SSDE covering 95% of the population for nD_{lung} with 95% confidence was observed to be 35.6%.

Figure 5B shows nD_{breast} parameterized as an exponential function with D_w in relation to SSDE. For nD_{breast}, $\Delta D_{SSDE,breast}$ values ranged from -90.8% to 10.4%. $\overline{\Delta D_{SSDE,breast}}$ was observed to be 31.8% and $\Delta S_{SSDE,breast}$ was observed to be 18.7%. Of the 85 cases, 26 of the nD_{breast} values were within 20% of SSDE (C_p = 30.6%) while 44 of the nD_{breast} values were within 30% of SSDE (C_p = 51.8%). 41 of the nD_{breast} cases were beyond 30% of SSDE (C_p = 48.2%). Using N = 85, T_U for SSDE covering 95% of the population for nD_{breast} with 95% confidence was observed to be 60.7%. **Table 7** contains the summary statistics for nD_{lung} and nD_{breast} values relative to the SSDE and the T_U for each organ. **Table 10** contains the frequency table for nD_{lung} and nD_{breast} values relative to 20% and 30% of the SSDE.

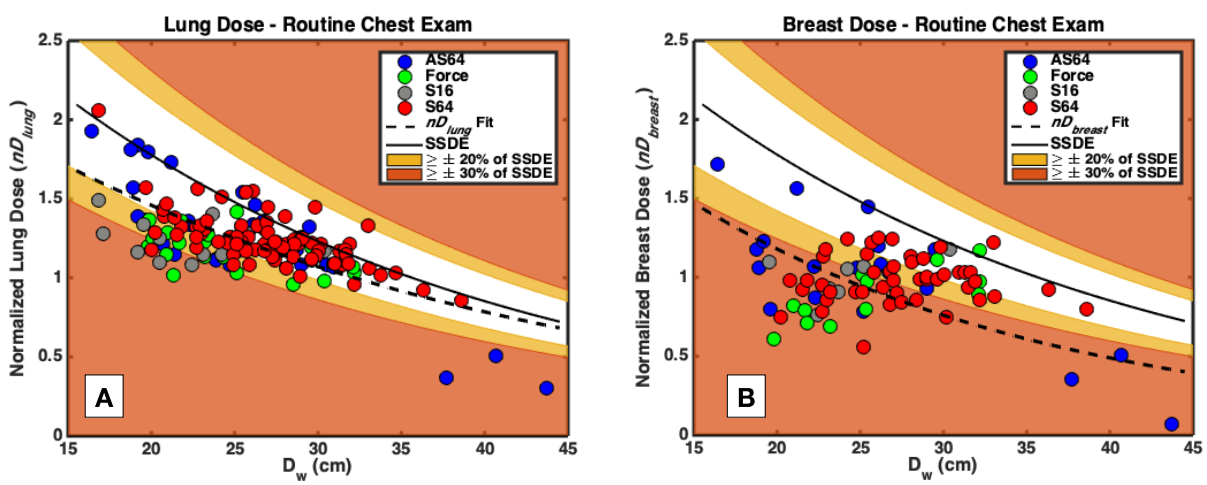

Figure 5: A) nD_{lung} and **B)** nD_{breast} values in relation to SSDE from AAPM Report 204 with shaded areas corresponding to ± 20% and ± 30% of the SSDE

Table 7: Summary statistics for nD_{lung} and nD_{breast} values relative to SSDE and the T_U for each estimate of normalized lung dose

	nD_{lung}	nD_{breast}
$\Delta D_{SSDE,organ}$ range (%)	-60.4 to 20.1	-90.8 to 10.4
$\overline{\Delta D_{SSDE,organ}}$ (%)	15.3	31.8
$\Delta S_{SSDE,organ}$ (%)	10.9	18.7
T_U (%)	35.6	68.3

Table 8: Frequency table of nD_{lung} and nD_{breast} relative to SSDE from routine TCM chest exams

	nD_{lung} (N=160)	nD_{breast} (N=85)
within ± 20% of SSDE	119 C_p = 74.4%	26 C_p = 30.6%
within ± 30% of SSDE	148 C_p = 92.5%	44 C_p = 51.8%
beyond ± 30% of SSDE	12 C_p = 7.5%	41 C_p = 48.2%

3.C SSDE relative to liver, spleen, and kidney dose from routine abdominal/pelvis exams

Figure 6A contains nD_{liver} parameterized as an exponential function with D_w in relation to SSDE from AAPM Report 204. $\Delta D_{SSDE,liver}$ values ranged from -54.0% to 28.7%. $\overline{\Delta D_{SSDE,liver}}$ was observed to be 13.1% and $\Delta S_{SSDE,liver}$ was observed to be 9.2%. Of the 107 cases, 88 of the nD_{liver} values were within 20% of SSDE (C_p = 82.2%) while 104 of the nD_{liver} values were within 30% of the SSDE (C_p = 97.2%). Only 3 of the nD_{liver} cases were beyond 30% of SSDE (C_p = 2.8%). Using N = 107, T_U for SSDE covering 95% of the population for nD_{liver} with 95% confidence was observed to be 30.7%.

Figure 6B contains nD_{spleen} parameterized as an exponential function with D_w in relation to SSDE from AAPM Report 204. $\Delta D_{SSDE,spleen}$ values ranged from -44.4% to 35.4%. $\overline{\Delta D_{SSDE,spleen}}$ was observed to be 14.1% and $\Delta S_{SSDE,spleen}$ was observed to be 10.0%. Of the 107 cases, 81 of the nD_{spleen} values were within 20% of SSDE (C_p = 75.7%) while 99 of the nD_{spleen} values were within 30% of SSDE (C_p = 92.5%). Only 8 of the nD_{spleen} cases were beyond 30% of SSDE (C_p = 7.5%). T_U for SSDE covering 95% of the population for nD_{spleen} with 95% confidence was observed to be 33.2%.

Figure 6C contains nD_{kidney} parameterized as an exponential function with D_w in relation to SSDE from AAPM Report 204. $\Delta D_{SSDE,kidney}$ values ranged from -49.6% to 47.3%. $\overline{\Delta D_{SSDE,kidney}}$ was observed to be 13.7% and $\Delta S_{SSDE,kidney}$ was observed to be 10.1%. Of the 107 cases, 83 of the nD_{kidney} values were within 20% of SSDE (C_p = 77.6%) while 100 of the nD_{kidney} values were within 30% of the SSDE (C_p = 93.5%). Only 7 of the nD_{kidney} cases were beyond 30% of SSDE (C_p = 6.5%). T_U for the SSDE covering 95% of the population for nD_{kidney} with 95% confidence was observed to be 33.0%. **Table 9** contains the summary statistics for nD_{liver}, nD_{spleen}, and nD_{kidney} values relative to the SSDE and the T_U for each organ. **Table 10** contains the frequency table for nD_{liver}, nD_{spleen}, and nD_{kidney} values relative to 20% and 30% of SSDE.

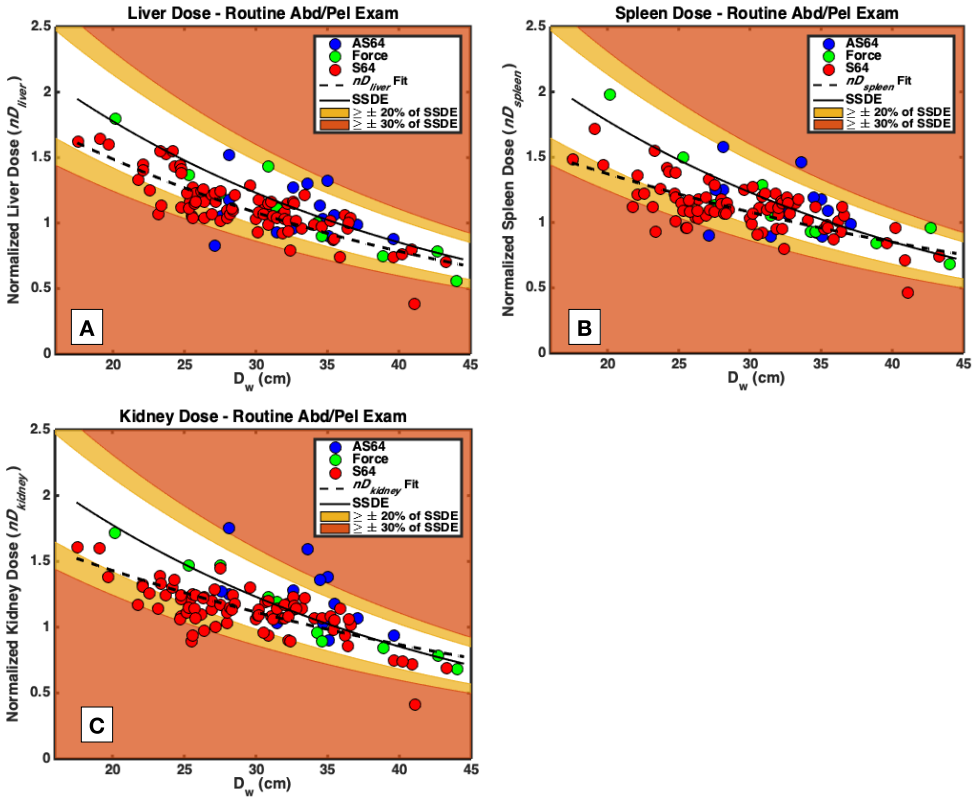

Figure 6: A) nD_{liver}, **B)** nD_{spleen}, and **C)** nD_{kidney} values in relation to SSDE from AAPM Report 204 with shaded areas corresponding to ± 20% and ± 30% of the SSDE

Table 9: Summary statistics for nD_{liver}, nD_{spleen}, and nD_{kidney} values relative to SSDE and the T_U for each organ for TCM abdomen/pelvis exams

	nD_{liver}	nD_{spleen}	nD_{kidney}
$\Delta D_{SSDE,organ}$ range (%)	-54.0 to 28.7	-44.4 to 35.4	-49.6 to 47.3
$\overline{\Delta D_{SSDE,organ}}$ (%)	13.1	14.1	13.7
$\Delta S_{SSDE,organ}$ (%)	9.2	10.0	10.1
T_U (%)	30.7	33.2	33.0

Table 10: Frequency table of nD_{liver}, nD_{spleen}, and nD_{kidney} relative to SSDE from routine TCM abdominal/pelvis exams

	nD_{liver} (N=107)	nD_{spleen} (N=107)	nD_{kidney} (N=107)
within ± 20% of SSDE	88 C_p = 82.2%	81 C_p = 75.7%	83 C_p = 77.6%
within ± 30% of SSDE	104 C_p = 97.2%	99 C_p = 92.5%	100 C_p = 93.5%
beyond ± 30% of SSDE	3 C_p = 2.8%	8 C_p = 7.5%	7 C_p = 6.5%

4. DISCUSSION

In this study, SSDE was compared to organ dose estimates from validated, direct MC simulation methods for three routine CT examinations across a wide range of patient sizes that included pediatric patients, adult patients, and, for the body scans, bariatric patients. The framework for evaluation, specifically for those exams using TCM, is outlined in **Figure 3**. The routine examinations included head exams performed with FTC, chest and abdomen/pelvis exams performed with TCM. Unlike the Moore et al. and Sinclair et al. studies mentioned previously, this study used D_w estimates taken either from patient topograms or image data to calculate the SSDE as opposed to the geometric size descriptor of *ED*. Moreover, this study directly evaluated SSDE on a per-organ basis with the aim of providing an upper tolerance limit for which SSDE will cover 95% of the population (p = 0.95) with 95% confidence (α = 0.05) for a particular organ. Lastly, the evaluation of the SSDE was performed to test if the $T_U \leq 20\%$ between SSDE and patient dose as noted in AAPM Report 204.

For routine FTC head exams, this study observed that the T_U for the difference between nD_{brain} and SSDE from AAPM 293 needed to cover 95% of the population with 95% confidence was 12.5%. Additionally, as can be seen in **Figure 4**, all 15 nD_{brain} values were within 20% of SSDE (C_p = 100.0%). This suggests that the T_U of 20% between SSDE and patient dose noted in AAPM Report 204 may be appropriate for routine head CT examinations employing FTC and that SSDE may serve as a good estimate for brain parenchyma dose to within 12.5% for at least 95% of the population. There are two explanations for this observation. The first is that SSDE reported in both AAPM Reports 293 and 204 were derived from FTC measurements and simulations [11], [12]. The second explanation is related to the fact that, as noted in Hardy et al. [18], the head is composed of homogenous tissue encased in bone, which SSDE in AAPM Report 293 took into consideration. Thus, as can be seen again in **Figure 4**, the nD_{brain} as a function of D_w follows the SSDE curve, the average difference between them being less than 5% ($\overline{\Delta D_{SSDE,brain}}$ = 4.4%) with $\Delta S_{SSDE,brain}$ of only 3.2%. AAPM Report 293 does not explicitly note the same ±20% difference between SSDE and patient dose (brain parenchyma dose in this case) as in AAPM Report 204 [11], [12]. AAPM Report 293, however, is an extension of AAPM Report 204 [11], [12].

For routine chest, this study evaluated SSDE against both $CTDI_{vol,32}$-normalized lung and breast doses. This study observed that, when using $CTDI_{vol,32}$ as the normalization for lung dose, the T_U for the difference between nD_{lung} and SSDE needed to cover 95% of the population with 95% confidence was 35.6%. This result suggests that the 20% difference between SSDE and patient dose noted in AAPM Report 204 might not be sufficient for SSDE to cover 95% of nD_{lung} cases from routine chest exams employing TCM. Rather, the results of this study suggest that a wider tolerance may be needed in order for SSDE to serve as an estimate of lung dose. One possible reason for this has to do with the longitudinal modulation provided by CAREDose4D. In terms of dose reduction, TCM has been shown to reduce lung and breast dose relative to FTC in chest exams [29]. Because of the lower overall normalized dose provided by TCM relative to FTC, SSDE, as can be seen in **Figure 5A**, are a conservative estimate of nD_{lung}, with the vast majority of the data points falling within 30% of SSDE (C_p = 92.5%). Additionally, as can also be seen in **Figure 5A**, nD_{lung} values and regression fits tend to track closer to SSDE with

increasing D_w, most probably due to the response of the AEC system of maxing out tube current output for larger-sized patients. **Figure 7** below shows the TCM profile of a non-bariatric and a bariatric patient administered a routine chest exam. In **Figure 7B**, this TCM profile has very little longitudinal modulation due to the attenuation characteristics of the patient. Although the number of bariatric patients in this study was limited, this trend may nevertheless suggest different regimes within the normalized dose curves in relation to tube output potential of a scanner and patient size.

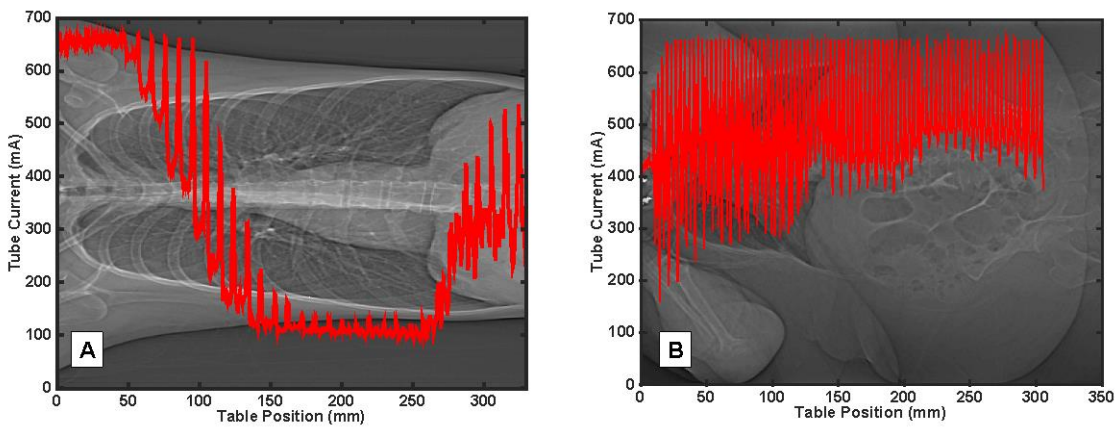

Figure 7: Examples of TCM profile from a routine chest exam of a **A)** typical, non-bariatric patient and **B)** bariatric patient. In **B)**, longitudinal modulation is minimal due to patient size and tube current limitation.

This study observed that the T_U for the difference between nD_{breast} and SSDE needed to cover 95% of the population with 95% confidence was observed to be 68.3%. These observations can be seen more clearly in **Figure 5B** for nD_{breast}. nD_{breast} values, as well as the corresponding regression fits between nD_{breast} and D_w, were systematically below SSDE with only a few exceptions (nD_{breast}: $\overline{\Delta D_{SSDE,breast}}$ = 31.8%, $\Delta S_{SSDE,breast}$ = 18.7%). As was seen in the lung, the normalized breast dose from TCM is systematically smaller than SSDE. Thus, this study suggests that SSDE may be a conservative estimate for nD_{breast} for most of the population. A tolerance wider than the 20% difference between patient dose and SSDE specified in AAPM Report 204 would be needed to encompass 95% with 95% confidence of nD_{breast}.

For abdomen/pelvis exams, this study found that that the T_U for the difference between nD_{liver}, nD_{spleen}, and nD_{kidney} and SSDE needed to cover 95% of the population with 95% confidence was 30.7%, 33.2%, and 33.0%, respectively. These results indicate that a tolerance wider than a 20% difference between SSDE and $CTDI_{vol,32}$-normalized organ dose would be needed to capture 95% of nD_{liver}, nD_{spleen}, and nD_{kidney} cases with 95% confidence. These results are illustrated in the **Figure 6** for nD_{liver}, nD_{spleen}, and nD_{kidney}, respectively, wherein, for all three organs, the vast majority of the nD_{liver}, nD_{spleen}, and nD_{kidney} cases are within 30% of SSDE ($C_p = 97.2\%$, $C_p = 92.5\%$, and $C_p = 93.5\%$, respectively). Additionally, as can be seen in **Table 9**, all three of these organs had fairly similar deviations from SSDE as indicated by the proximity of their $\overline{\Delta D_{SSDE,organ}}$ and $\Delta S_{SSDE,organ}$ values to one another. Given this, an equivalent T_U for these three organs of the abdomen/pelvis is a reasonable result.

A general trend was observed that normalized doses from TCM protocols were lower than SSDE. This observation is intuitive given that TCM reduces normalized dose relative to FTC [29]. The data suggests that another model of normalized dose that takes into consideration the effects of TCM may be needed. A potential candidate for such a dose model that considers TCM is the generalized linear model (GLM) developed by Bostani et al. [30]. The GLM is a statistical dose model that allows for the inclusion of categorical variables for different radiosensitive organs and scanners and was constructed with TCM MC simulations [30]. Given the widespread use of TCM, it is possible that normalized dose coefficients derived from GLM may be more appropriate in the current context of clinical practice. This, though, would require further investigation.

This study had a few advantages. This study capitalized on the strengths of the direct MC simulation approach to evaluate SSDE in light of organ dose estimates that are reflective of actual patient anatomy and actual, clinical TCM schemes. The evaluation of SSDE was performed on a per-organ basis using those MC-derived organ dose estimates across a range of patient sizes and across several routine protocols. Even given these advantages, however, this study nevertheless had a few limitations. For head exams, though the expectation is that brain parenchyma dose from FTC will not significantly deviate from SSDE, the sample sizes were nevertheless small because organ dose data was based on previous work.

Future work would involve using a large sample size to evaluate SSDE for the doses for this protocol. For those routine examinations employing TCM, which was the majority of the protocols investigated herein, only one AEC algorithm from one manufacturer, Siemens, was considered due to the lack of accessibility of complete TCM information from other scanner manufacturers. Future work would involve performing the direct simulation method with TCM information from other manufacturers and scanners. Additionally, though this study attempted to evaluate SSDE across a range of patient sizes, this study only contained a limited number of bariatric patients. Future work in this avenue would involve the incorporation of more bariatric patients in the evaluation of SSDE.

5. CONCLUSION

This study evaluated SSDE as an estimate of organ dose in light of organ dose estimates from direct MC simulation methods, using the 20% threshold mentioned in AAPM Report 204 as the point of departure for the evaluation. In the case of routine exams, with the exception of brain parenchyma doses routine FTC head exams, the null hypothesis of this study was rejected in that T_U was found to be greater than 20% for the organ doses investigated from body routine exams. Results indicate that a 20% threshold difference is most likely sufficient for 95% coverage of brain parenchyma dose cases from routine FTC head exams. For body exams using TCM, a threshold difference of ~30-36% would be wide enough to cover the majority (95%) of the organs investigated in this study, excluding the breasts, where SSDE serves as a conservative estimate.

REFERENCES

[1] F. A. Mettler *et al.*, “Radiologic and Nuclear Medicine Studies in the United States and Worldwide: Frequency, Radiation Dose, and Comparison with Other Radiation Sources—1950–2007,” *Radiology*, vol. 253, no. 2, pp. 520–531, 2009.

[2] R. Smith-Bindman *et al.*, “Radiation Doses in Consecutive CT Examinations from Five University of California Medical Centers,” *Radiology*, vol. 277, no. 1, pp. 134–141, May 2015.

[3] C. H. McCollough, S. Leng, L. Yu, D. D. Cody, J. M. Boone, and M. F. McNitt-Gray, “CT dose index and patient dose: they are not the same thing.,” *Radiology*, vol. 259, no. 2, pp. 311–316, 2011.

[4] Computerized Imaging Reference Systems Inc., “ATOM Dosimetry Verification Phantoms.” [Online]. Available: http://www.cirsinc.com/products/radiation-therapy/atom-dosimetry-verification-phantoms/. [Accessed: 30-Apr-2019].

[5] D. Zhang *et al.*, “In vitro dose measurements in a human cadaver with abdomen/pelvis CT scans,” *Med. Phys.*, vol. 41, no. 9, pp. 1–9, 2014.

[6] J. W. Mueller *et al.*, “In vivo CT dosimetry during CT colonography,” *Am. J. Roentgenol.*, vol. 202, no. 4, pp. 703–710, 2014.

[7] D. Zhang *et al.*, “Variability of surface and center position radiation dose in MDCT: Monte Carlo simulations using CTDI and anthropomorphic phantoms.,” *Med. Phys.*, vol. 36, no. 3, pp. 1025–38, 2009.

[8] W. P. Segars, M. Mahesh, T. J. Beck, E. C. Frey, and B. M. W. Tsui, “Realistic CT simulation using the 4D XCAT phantom.,” *Med. Phys.*, vol. 35, no. 8, pp. 3800–3808, 2008.

[9] AAPM Task Group 195, “Monte Carlo Reference Data Sets for Imaging Research,” College Park, MD, 2015.

[10] A. J. Hardy, M. Bostani, E. Angel, C. Cagnon, I. Sechopoulos, and M. F. McNitt-Gray, “Reference dataset for benchmarking fetal doses derived from Monte Carlo simulations of CT exams,” *Med. Phys.*, vol. n/a, no. n/a, Oct. 2020.

[11] AAPM Task Group 204, “Size-Specific Dose Estimates (SSDE) in Pediatric and Adult Body CT Examinations,” College Park, MD, Jan. 2011.

[12] AAPM Task Group 293, “Size-Specific Dose Estimate (SSDE) for Head CT: The Report of AAPM,” College Park, MD, 2019.

[13] B. M. Moore, S. L. Brady, A. E. Mirro, and R. A. Kaufman, “Size-specific dose estimate (SSDE) provides a simple method to calculate organ dose for pediatric CT examinations,” *Med. Phys.*, vol.

41, no. 7, pp. 1–10, 2014.

[14] T. M. Griglock *et al.*, “Determining Organ Doses from CT with Direct Measurements in Postmortem Subjects: Part 1—Methodology and Validation,” *Radiology*, vol. 277, no. 2, pp. 463–470, 2015.

[15] AAPM Task Group 220, “Use of Water Equivalent Diameter for Calculating Patient Size and Size-Specific Dose Estimates (SSDE) in CT,” College Park, MD, 2014.

[16] C. Lee, K. P. Kim, D. J. Long, and W. E. Bolch, “Organ doses for reference pediatric and adolescent patients undergoing computed tomography estimated by Monte Carlo simulation,” *Med. Phys.*, vol. 39, no. 4, pp. 2129–2146, 2012.

[17] X. Li *et al.*, “Patient-specific radiation dose and cancer risk estimation in CT: Part II. Application to patients,” *Med. Phys.*, vol. 38, no. 1, pp. 408–419, 2011.

[18] A. J. Hardy *et al.*, “Estimating a size-specific dose for helical head CT examinations using Monte Carlo simulation methods,” *Med. Phys.*, vol. 46, no. 2, pp. 902–912, Feb. 2019.

[19] N. Petoussi-Henss, M. Zankl, U. Fill, D. Regulla, and M. Zanki, “The GSF family of voxel phantoms,” *Phys. Med. Biol.*, vol. 47, no. 1, pp. 89–106, 2002.

[20] International Commission on Radiological Protection, “Adult reference computational phantoms,” *ICRP Publ. 110. Ann. ICRP 39*, vol. (2), 2009.

[21] M. Zankl, K. F. Eckerman, and W. E. Bolch, “Voxel-based models representing the male and female ICRP reference adult - The skeleton,” *Radiat. Prot. Dosimetry*, vol. 127, no. 1–4, pp. 174–186, 2007.

[22] J. J. Demarco, T. D. Solberg, and J. B. Smathers, “A CT-based Monte Carlo simulation tool for dosimetry planning and analysis,” *Med. Phys.*, vol. 25, pp. 1–11, 1998.

[23] M. Bostani *et al.*, “Accuracy of Monte Carlo simulations compared to in-vivo MDCT dosimetry.,” *Med. Phys.*, vol. 42, no. 2, p. 1080, 2015.

[24] E. Angel *et al.*, “Monte Carlo simulations to assess the effects of tube current modulation on breast dose for multidetector CT,” *Phys Med Biol*, vol. 54, no. 3, pp. 497–512, 2010.

[25] C. H. McCollough *et al.*, “Use of water equivalent diameter for calculating patient size and size-specific dose estimates (SSDE) in CT,” 2014.

[26] A. C. Turner *et al.*, “A method to generate equivalent energy spectra and filtration models based on measurement for multidetector CT Monte Carlo dosimetry simulations,” *Med. Phys.*, vol. 36, no. 6, 2009.

[27] J. J. DeMarco *et al.*, “A Monte Carlo based method to estimate radiation dose from multidetector CT (MDCT): cylindrical and anthropomorphic phantoms.,” *Phys. Med. Biol.*, vol. 50, no. 17, pp. 3989–4004, 2005.

[28] National Institute of Standards and Technology, “Engineering Statistics Handbook: Tolerance intervals for a normal distribution.” [Online]. Available: https://www.itl.nist.gov/div898/handbook/prc/section2/prc263.htm#cases. [Accessed: 28-Aug-2019].

[29] E. Angel *et al.*, “Dose to radiosensitive organs during routine chest CT: Effects of tube current modulation,” *Am. J. Roentgenol.*, vol. 193, no. 5, pp. 1340–1345, 2009.

[30] M. Bostani *et al.*, “Estimating organ doses from tube current modulated CT examinations using a generalized linear model,” *Med. Phys.*, vol. 44, no. 4, pp. 1500–1513, 2017.

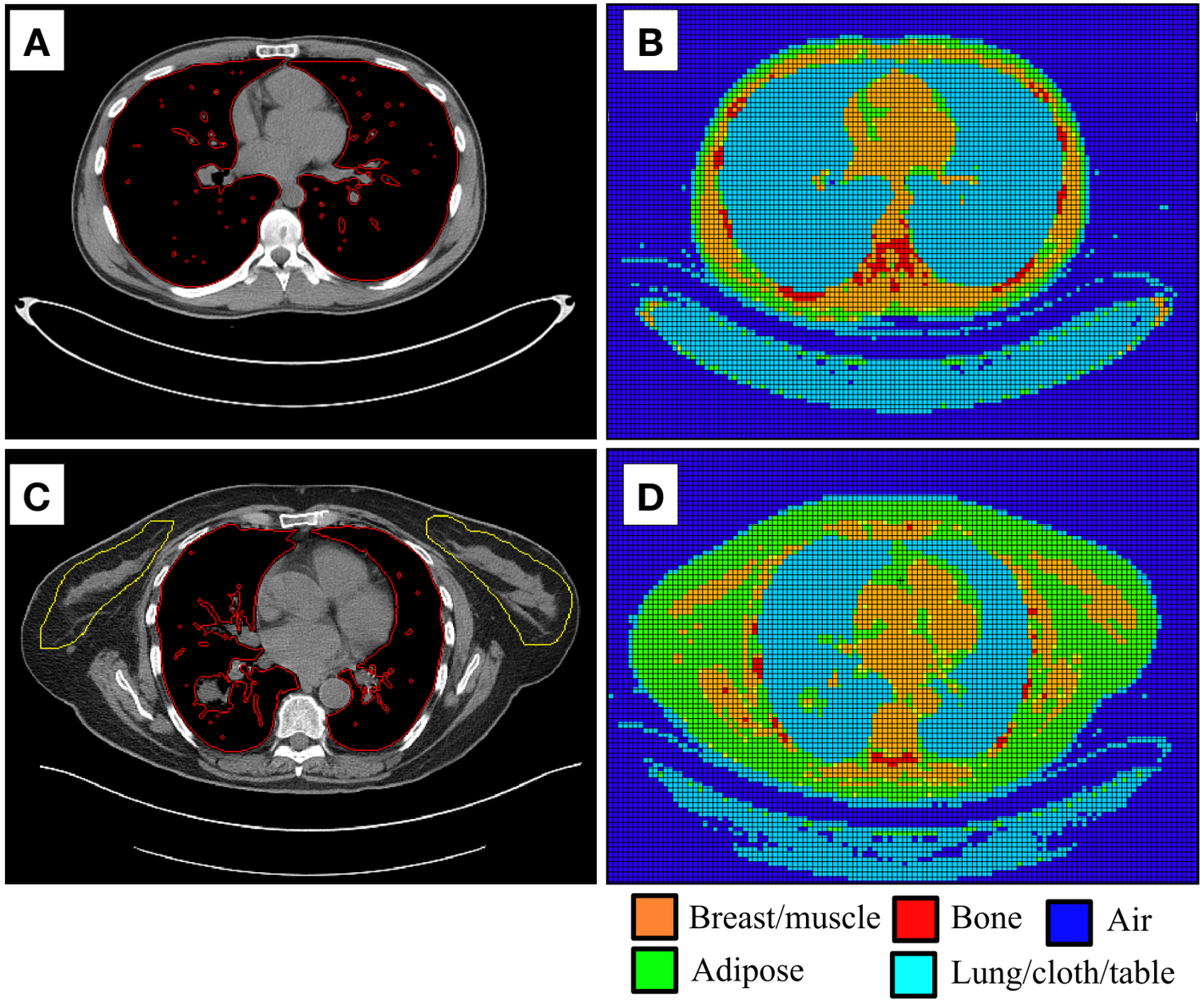
A
B
C
D
Breast/muscle
Bone
Air
Adipose
Lung/cloth/table

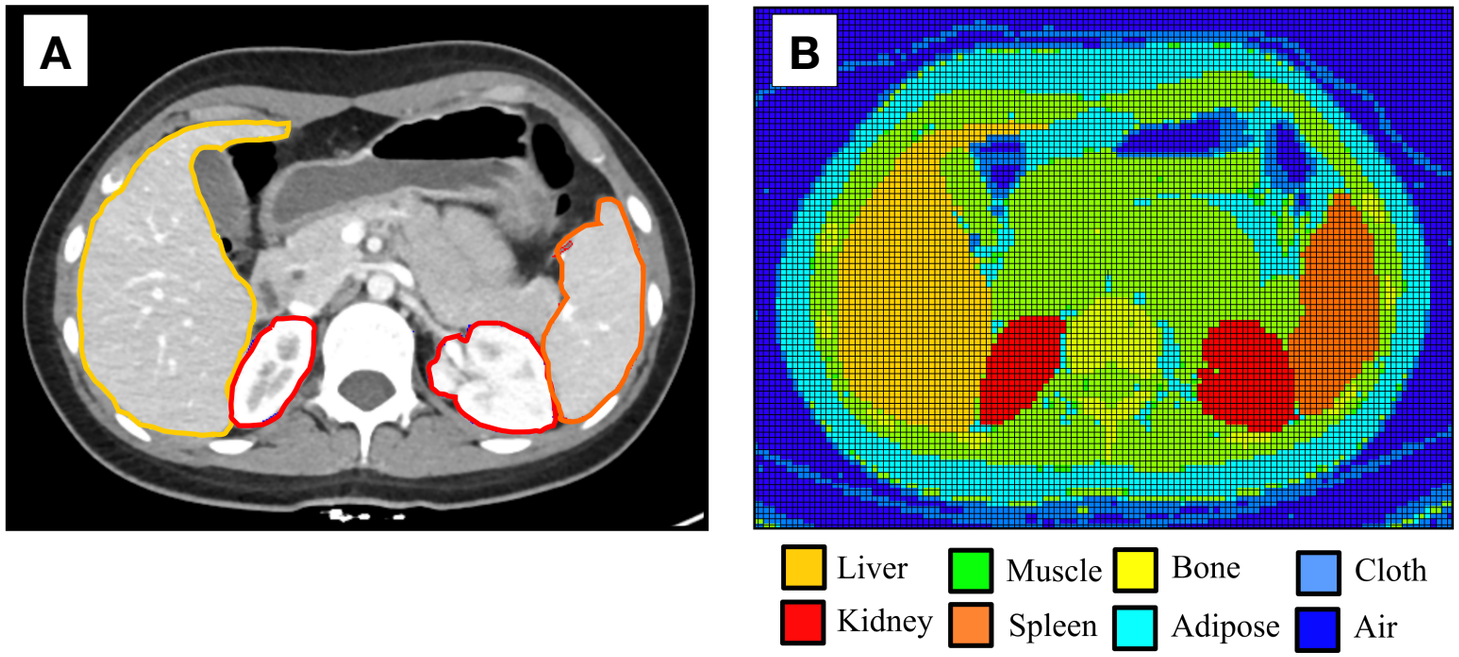
A
B
Liver
Muscle
Bone
Cloth
Kidney
Spleen
Adipose
Air

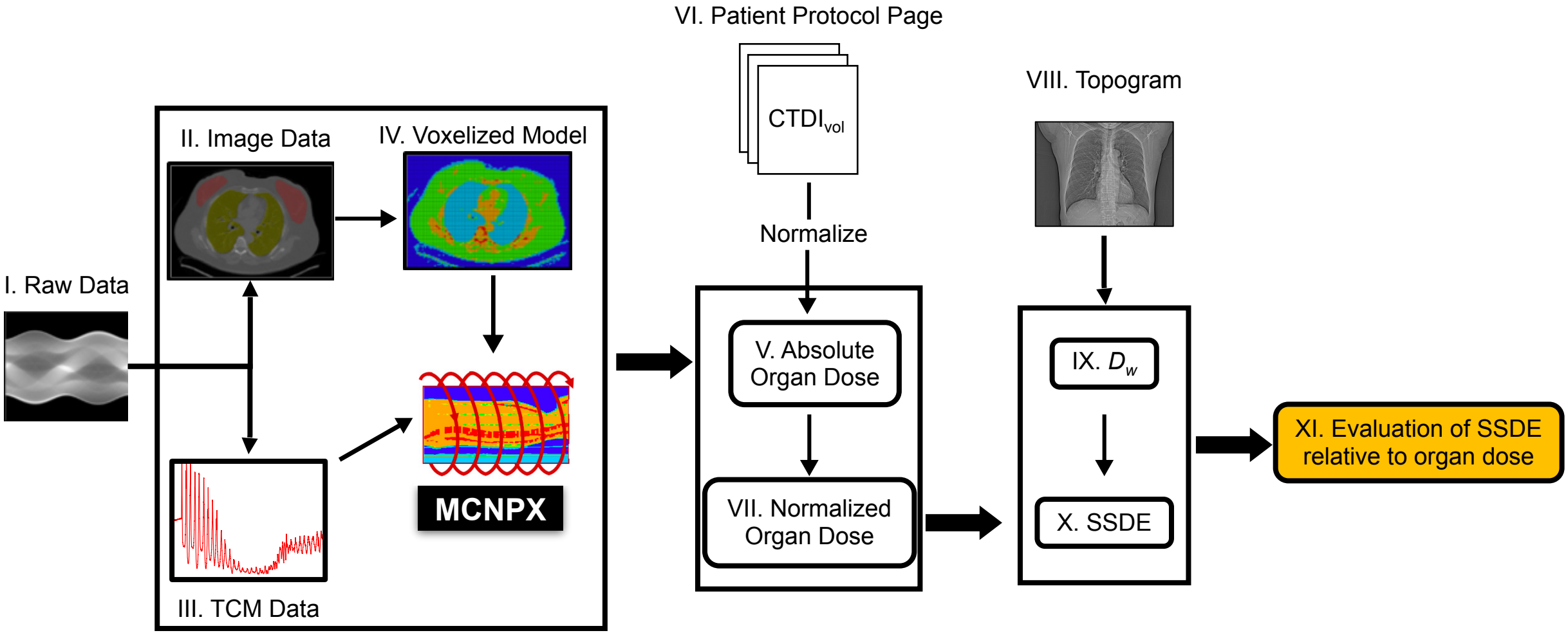
I. Raw Data
II. Image Data
III. TCM Data
IV. Voxelized Model
MCNPX
VI. Patient Protocol Page
CTDI$_{vol}$
Normalize
V. Absolute Organ Dose
VII. Normalized Organ Dose
VIII. Topogram
IX. D_w
X. SSDE
XI. Evaluation of SSDE relative to organ dose

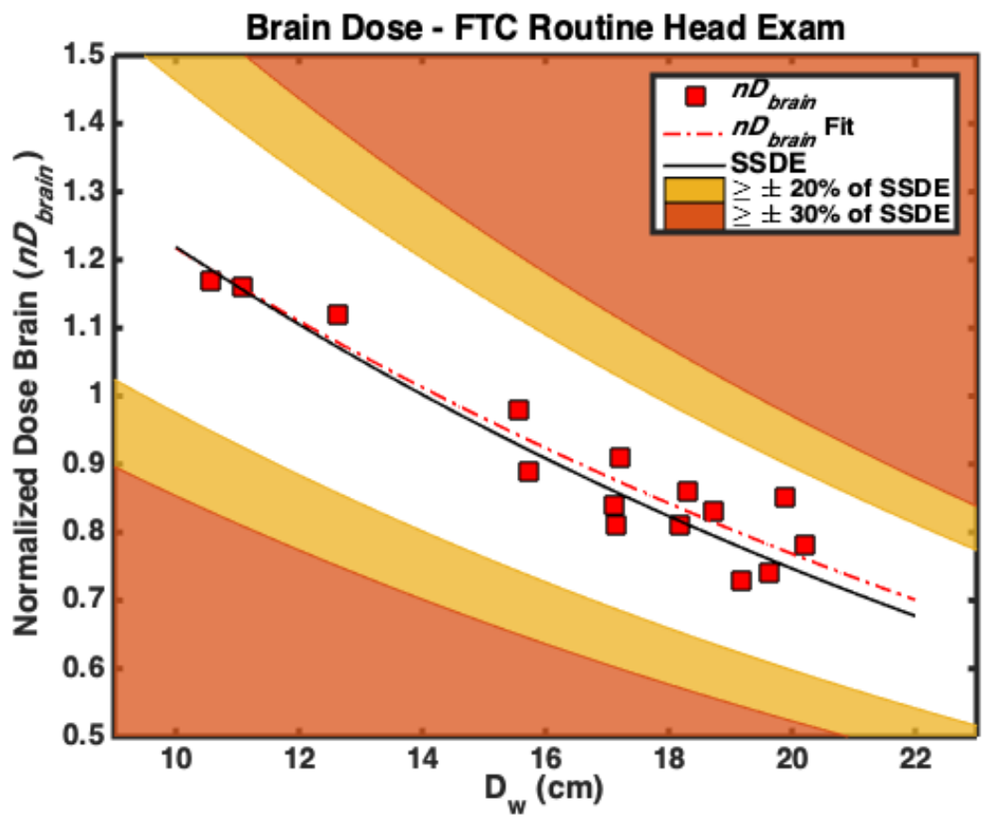
Brain Dose - FTC Routine Head Exam
Normalized Dose Brain (nD_{brain})
D_w (cm)
nD_{brain}
nD_{brain} Fit
SSDE
≥ ± 20% of SSDE
≥ ± 30% of SSDE
1.5
1.4
1.3
1.2
1.1
1
0.9
0.8
0.7
0.6
0.5
10
12
14
16
18
20
22

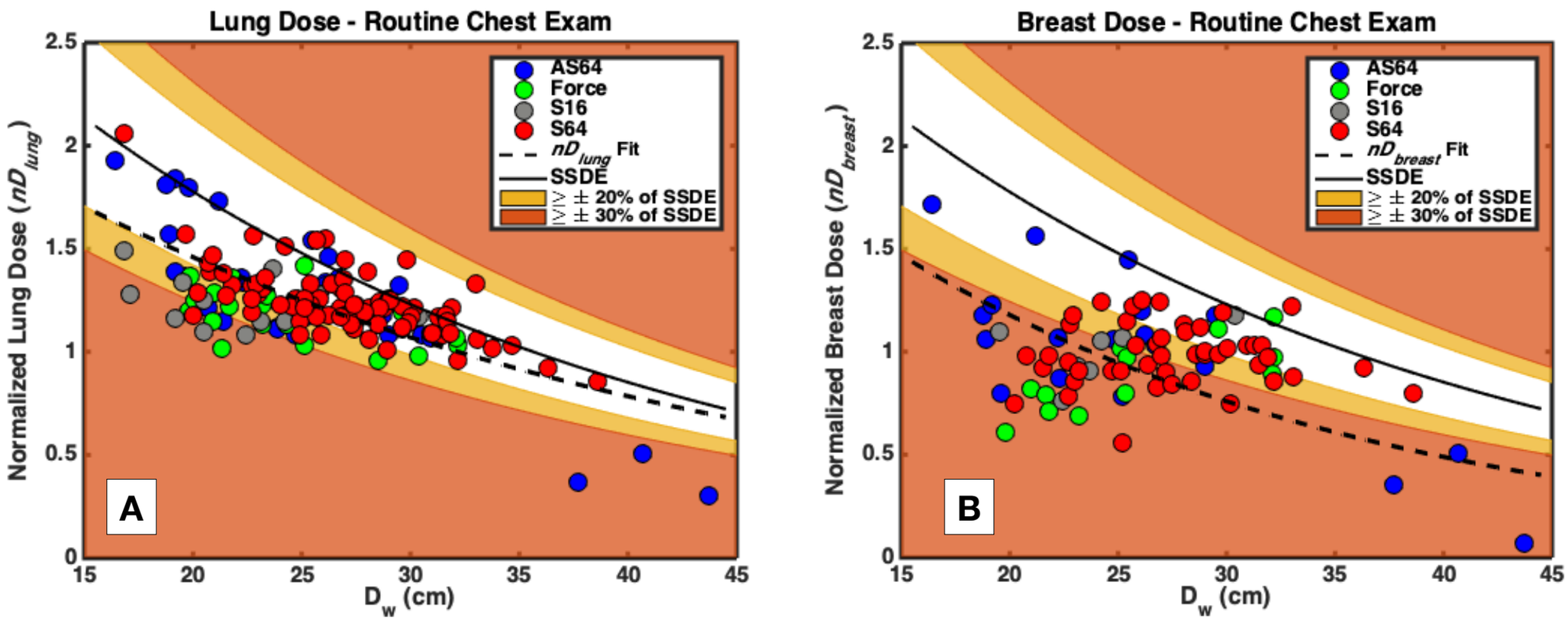
Lung Dose - Routine Chest Exam
Breast Dose - Routine Chest Exam
AS64
Force
S16
S64
nD lung Fit
nD breast Fit
SSDE
± 20% of SSDE
± 30% of SSDE
Normalized Lung Dose (nD lung)
Normalized Breast Dose (nD breast)
D w (cm)
A
B

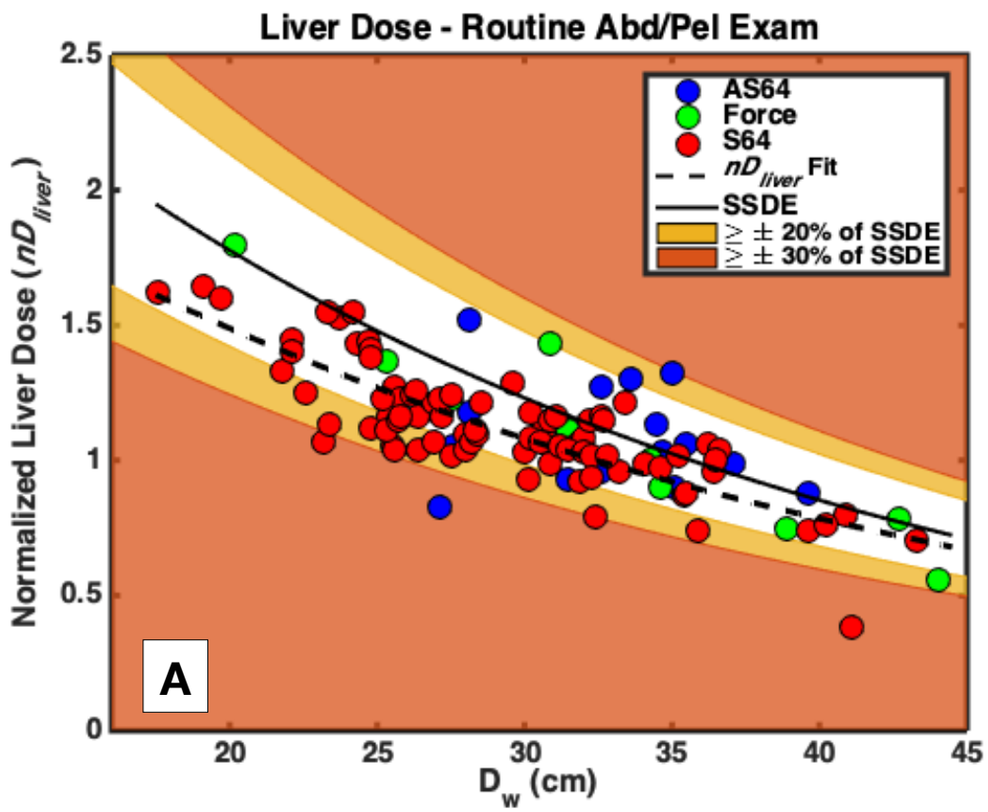
Liver Dose - Routine Abd/Pel Exam
AS64
Force
S64
nD_{liver} Fit
SSDE
≥ ± 20% of SSDE
≥ ± 30% of SSDE
A
Normalized Liver Dose (nD_{liver})
D_w (cm)

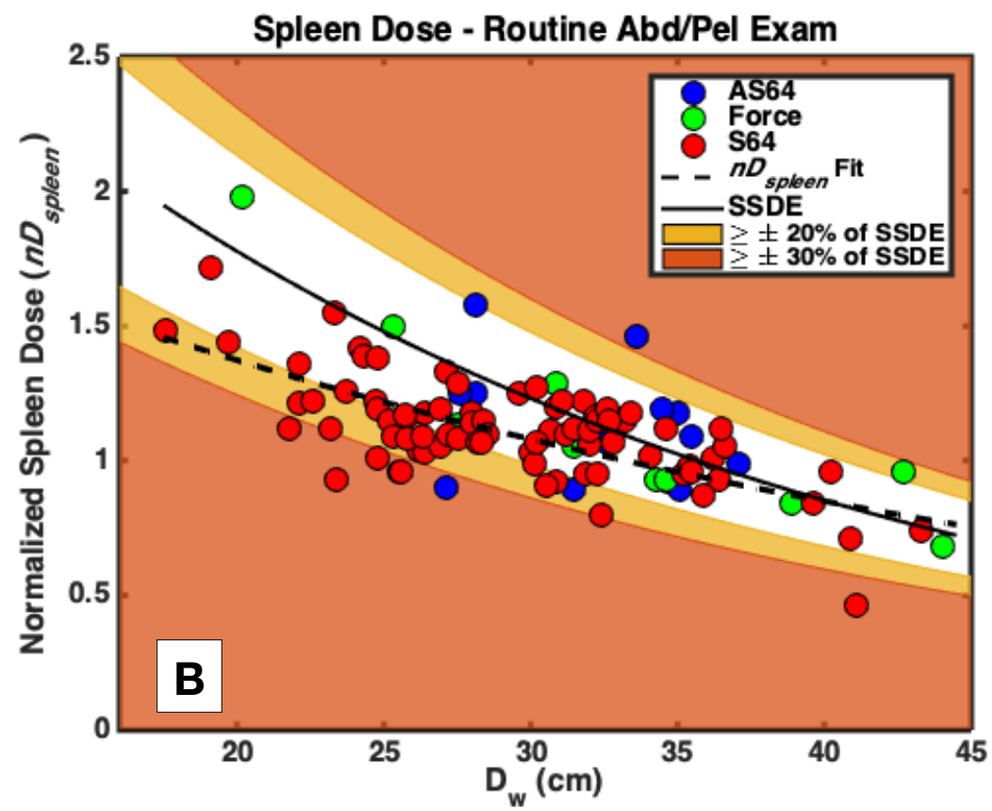
Spleen Dose - Routine Abd/Pel Exam
AS64
Force
S64
nD_{spleen} Fit
SSDE
≥ ± 20% of SSDE
≥ ± 30% of SSDE
B
Normalized Spleen Dose (nD_{spleen})
D_w (cm)

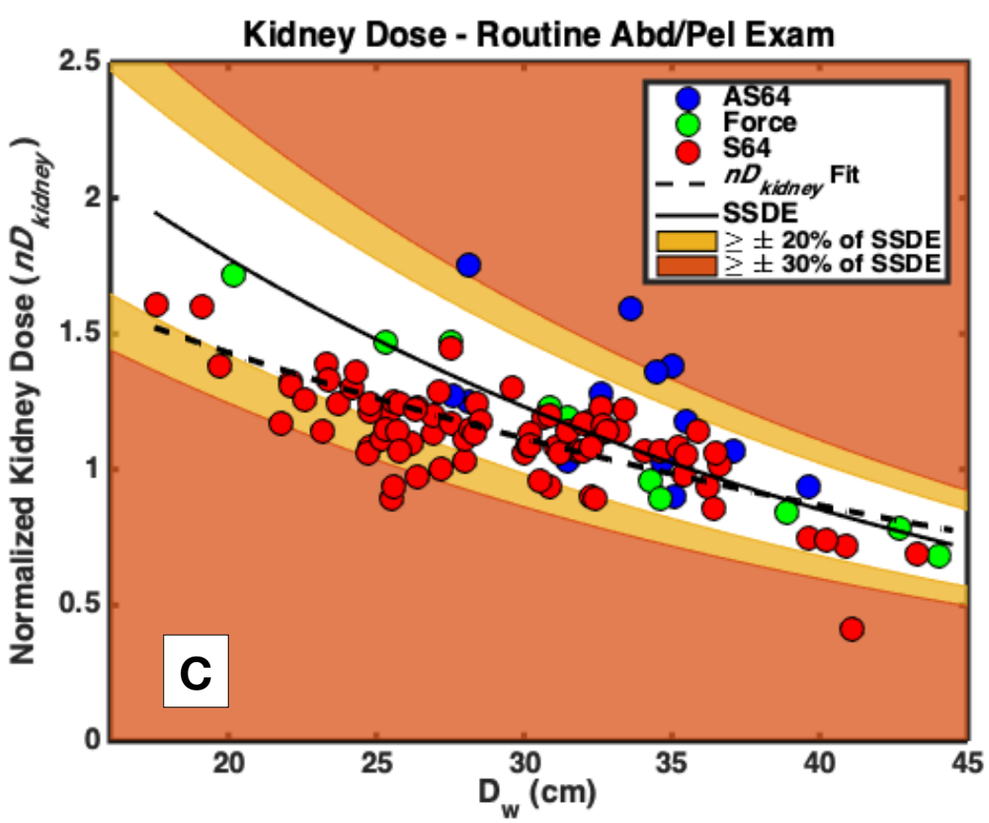
Kidney Dose - Routine Abd/Pel Exam
AS64
Force
S64
nD_{kidney} Fit
SSDE
≥ ± 20% of SSDE
≥ ± 30% of SSDE
C
Normalized Kidney Dose (nD_{kidney})
D_w (cm)

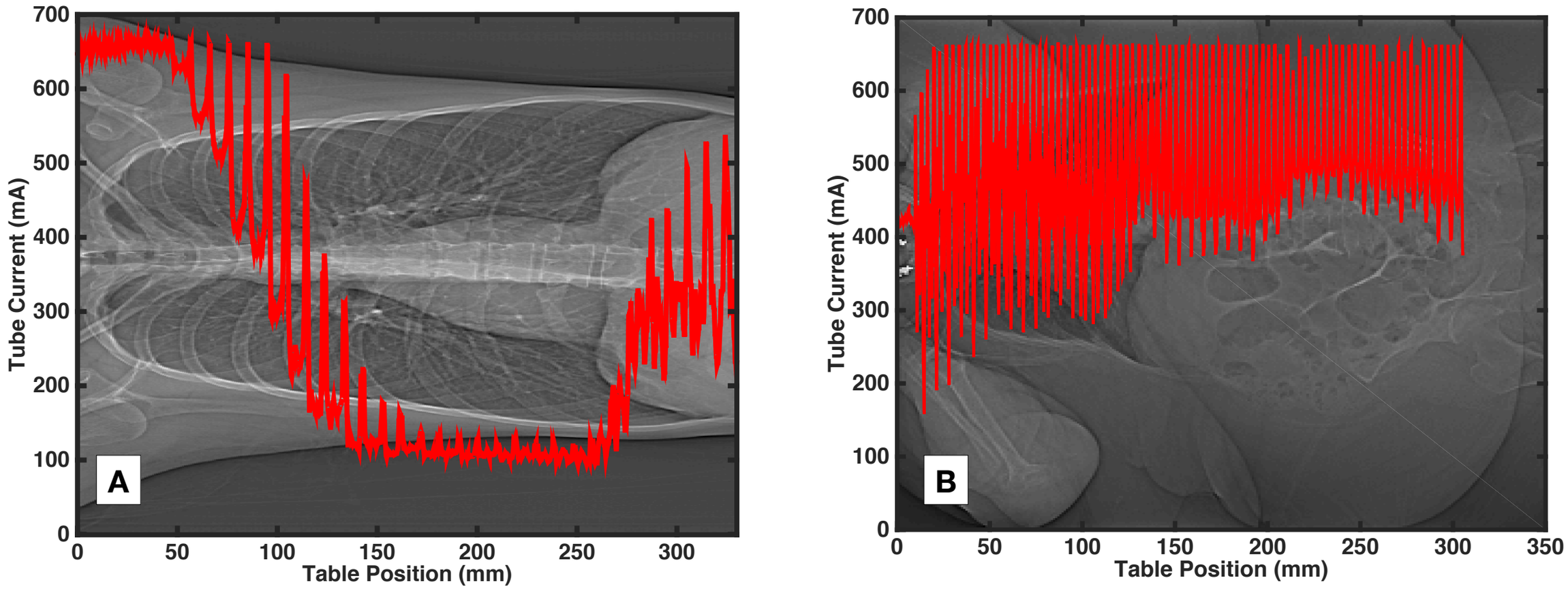
A
Tube Current (mA)
Table Position (mm)
0
100
200
300
400
500
600
700
0
50
100
150
200
250
300
B
Tube Current (mA)
Table Position (mm)
0
100
200
300
400
500
600
700
0
50
100
150
200
250
300
350